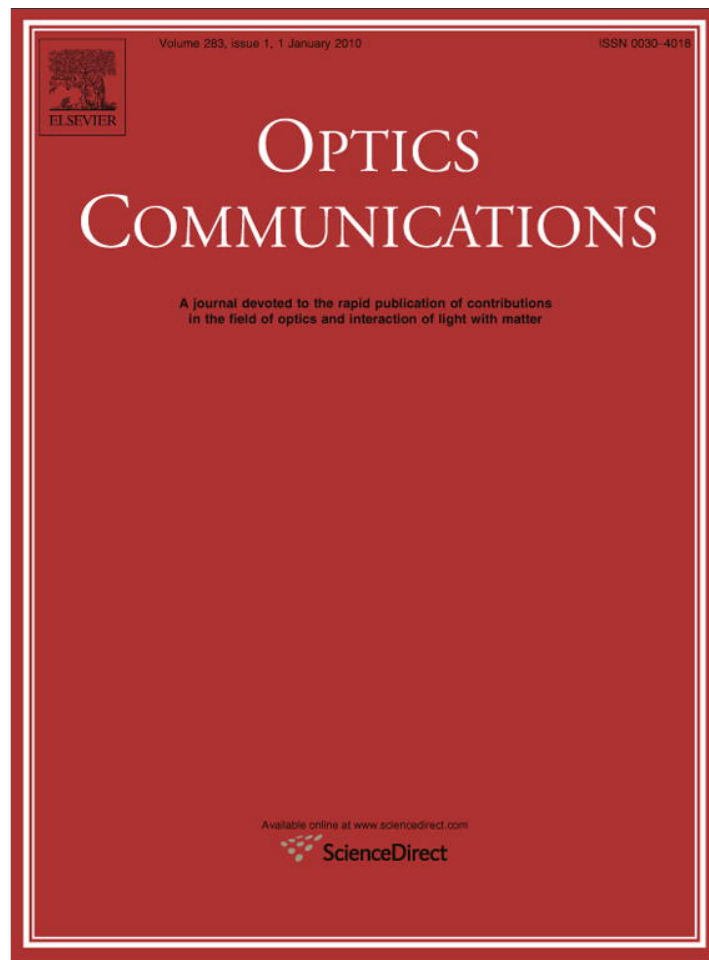


Provided for non-commercial research and education use.
Not for reproduction, distribution or commercial use.



This article appeared in a journal published by Elsevier. The attached copy is furnished to the author for internal non-commercial research and education use, including for instruction at the authors institution and sharing with colleagues.

Other uses, including reproduction and distribution, or selling or licensing copies, or posting to personal, institutional or third party websites are prohibited.

In most cases authors are permitted to post their version of the article (e.g. in Word or Tex form) to their personal website or institutional repository. Authors requiring further information regarding Elsevier's archiving and manuscript policies are encouraged to visit:

<http://www.elsevier.com/copyright>



Contents lists available at ScienceDirect

Optics Communications

journal homepage: www.elsevier.com/locate/optcom

Approach to extreme ultraviolet supercontinuum in a two-color laser field

Songsong Tang, Li Zheng, Xianfeng Chen *

Institute of Optics and Photonics, Department of Physics, The State Key Laboratory on Fiber Optic Local Area Communication Networks and Advanced Optical Communication Systems, Shanghai Jiao Tong University, 800 Dongchuan Rd., Shanghai 200240, China

ARTICLE INFO

Article history:

Received 27 July 2009

Received in revised form 29 September 2009

Accepted 29 September 2009

PACS:

32.80.Rm

42.65.Ky

42.65.Re

Keywords:

HHG

Two-color field

Supercontinuum

ABSTRACT

In recent years, it has been shown that an intense few-cycle driving pulse combined with a weak control pulse could efficiently extend the harmonic spectrum in the generation of high-order harmonics (HHG). In this paper, we adjust the intensities of the driving and control pulse to generate broader extreme ultraviolet (XUV) supercontinuum. We find that in some special situation when the intensity of the control pulse equals to that of the driving pulse, a clean supercontinuum as long as 80 eV can be realized and a 53-as pulse can be straightforwardly obtained.

© 2009 Elsevier B.V. All rights reserved.

1. Introduction

As we know, the vibrational oscillation period in hydrogen is about 7 femtoseconds (fs), and the Bohr-orbit time in hydrogen of the ground state is about 152 attoseconds (as). For the purpose of detecting and controlling the electronic dynamics inside atoms, an isolated attosecond pulse is an important tool. Currently, high-order harmonic generation from a few-cycle driving pulse [1] and temporal confinement of the HHG by polarization-gating [2] provide two ways to gain ultrafast XUV pulses. For the first approach, the more significantly the electric field amplitude varies from one half-optical cycle to the next, the higher the corresponding kinetic energy of an electron returning to its parent ion compared with that of other half-optical cycles in the few-cycle field [3], the maximum kinetic energy adding the ionization potential of the atom comes to the cutoff photon energy. The difference between the highest and the second highest cutoff photon energy (cutoff region) of different half-optical cycles is proportional to the bandwidth of the XUV supercontinuum [4] which could support an isolated attosecond pulse. In recent years, theoretical simulations show that two-color laser fields could efficiently modulate the kinetic energy of the active electron [5] and broaden the XUV

supercontinuum because the difference between the highest and the second highest cutoff photon energy of different half-optical cycles could be enlarged by superimposing a second-harmonic wave onto the driving pulse [6,7]. A few-cycle-800 nm pulse supports harmonic spectrum with a clean cutoff region and usually acts as the driving pulse. A weak control pulse is introduced to select a certain quantum path and restrain others of the driving pulse while remain the feature of the harmonic spectrum. In this paper, we ignore all quantum paths of the driving pulse and optimize the intensities of the driving and control pulse to gain the desired HHG spectrum with a clean and long cutoff region.

2. Optimizing method

In order to demonstrate our scheme, we first investigate the HHG process in terms of the semiclassical three-step model, which presents a clear physical picture. In our simulation, a 6 fs–800 nm pulse serves as the driving pulse. The synthesized two-color field is expressed as [8]

$$E_s = E_1 \exp[-2 \ln(2)t^2/\tau_1^2] \cos(\omega_1 t) + E_2 \exp[-2 \ln(2)(t + t_0)^2/\tau_2^2] \times \cos[\omega_2(t + t_0)], \quad (1)$$

here, E_1 and E_2 are the amplitudes of the electric field of the driving and the control pulse respectively; ω_1 and ω_2 are the frequencies of

* Corresponding author. Tel.: +86 21 54743252; fax: +86 21 54743273.
E-mail address: xfchen@sjtu.edu.cn (X. Chen).

the driving and the control pulse respectively; τ_1 and τ_2 are the pulse durations (FWHM) of the driving and the control pulse respectively; t_0 defines the time delay between the driving and the control pulse. Here we set $\omega_1 = 0.057$ a.u. corresponding to 800 nm, $\omega_2 = 0.338$ a.u. corresponding to 4750 nm, $\tau_1 = 6$ fs, $\tau_2 = 36$ fs, and $t_0 = 0$ fs. We define β as the intensity ratio between the two pulses ($\beta = E_2/E_1$).

The atom we used is helium (He) and our simulation is based on the single-active atom approximation. We adjust the intensities of the driving and the control pulse in binary system and use the simulated annealing (SA) method to optimally enlarge the difference between the highest and the second highest kinetic energy. The kinetic energy is set as $E_{kin}(t) = \max\{\int_{t_p}^t E_s(t) dt\}^2/2$ and the objective function is chosen as $F = \max(E_{kin}) - \text{second max}(E_{kin})$. In each step, a bit is randomly chosen and overturned (1 becomes 0 and 0 becomes 1). If the objective function F is enlarged, the bit

is confirmed; else the bit is confirmed in probability of $\exp(\frac{\Delta F}{T})$ (T is the temperature). Then turn to next step. After each step, the temperature is reduced. If no larger F appears in consecutive 100 steps, the program will be stopped.

3. Results and discussion

I_1 and I_2 are the intensities of the driving and the control pulse respectively. We remain $I_1 + I_2 = 1.0 \times 10^{14}$ W/cm² and adjust β from 0 to 2 with an interval of 0.01. By using the SA method, we find that when β equals to 1, our objective function comes to the maximum. The other parameters of the control pulse are confirmed in the same way. To see how β affects our objective function, we show the dependence of the kinetic energy with different β in Fig. 1 (black solid line for $\beta = 0$, magenta dash dot line for $\beta = 0.5$, red dash line for $\beta = 1$, blue dot line for $\beta = 2$, green dash dot dot line for $E_1 = 0$). Each peak represents one quantum path, for $\beta = 1$ (red dash line), electrons recombine near three peaks A, B and C will emit XUV photons of the highest energy. The highest part of peak B above peak C (cutoff region) is about 80 eV. For each peak, the left and the right arm represent the short and the long electron trajectory respectively. For the highest peak, shorter time interval between the left and the right arm represents less phase slip and a cleaner HHG spectrum.

The HHG spectrums of the synthesized two-color pulse are shown in Fig. 2a (black line for $\beta = 0$, gray line for $\beta = 0.5$, light gray line for $\beta = 1$) and Fig. 2b (black line for $\beta = 1$, gray line for $\beta = 2$, light gray line for $E_1 = 0$). We could see that the kinetic energy curves in Fig. 1 match the HHG spectrums in Fig. 2a and b quite well. For $\beta = 1$, the high sharp peak B (red dash line in Fig. 1) leads to HHG spectrum with high cutoff energy and a broadband flat supercontinuum cutoff region with little spectral modulation (light gray line in Fig. 2a and black line in Fig. 2b).

The physical picture behind is that a proper combine of the driving and the control pulse mostly modulate the electron dynamics [9,10]. For a single color pulse, the ponderomotive energy of the electron is $U_p = E^2/4\omega^2$ and the maximum of the cutoff region is about $3.2U_p$. With higher intensity or lower frequency, the electron will gain more energy. For a two-color pulse, the classical velocity v of the electron is

$$v = - \int [E_1(t) + E_2(t)] dt = v_1 + v_2, \quad (2)$$

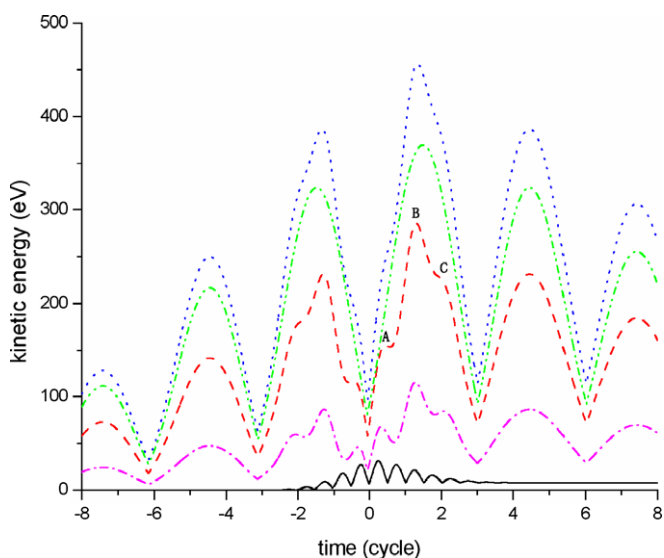


Fig. 1. The dependence of the kinetic energy on the recombination times of the synthesized two-color pulse (black solid line for $\beta = 0$, magenta dash dot line for $\beta = 0.5$, red dash line for $\beta = 1$, blue dot line for $\beta = 2$, green dash dot line for $E_1 = 0$). (For interpretation of the references to color in this figure legend, the reader is referred to the web version of this article.)

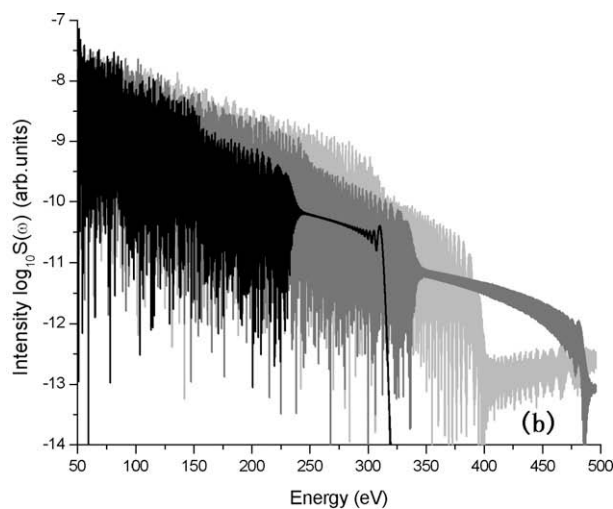
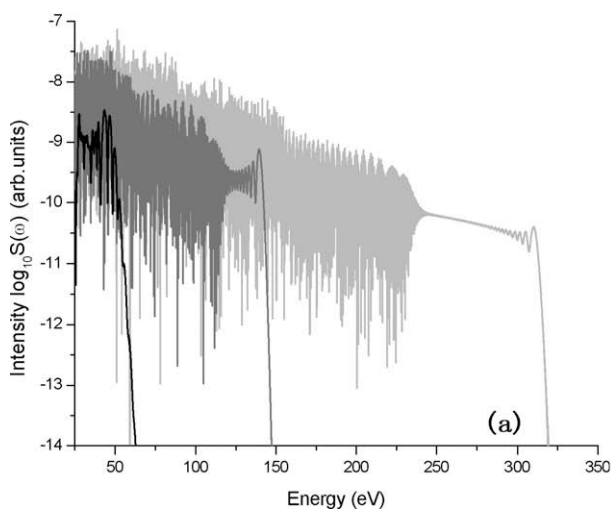


Fig. 2. (a) The harmonic spectrum of the synthesized two-color pulse (black line for $\beta = 0$, gray line for $\beta = 0.5$, light gray line for $\beta = 1$). (b) The harmonic spectrum of the synthesized two-color pulse (black line for $\beta = 1$, gray line for $\beta = 2$, light gray line for $E_1 = 0$).

The kinetic energy is

$$E_{kin} = \frac{1}{2}(v_1 + v_2)^2 = \frac{1}{2}(v_1^2 + v_2^2 + 2v_1v_2), \quad (3)$$

We believe that larger kinetic energy could be gained if $E_1(t)$ and $E_2(t)$ are optimized properly. In the generation of high-order harmonics, only those electrons born at time t_b and return to the parent ions at time t in the same position will emit HHG. Here t_b and t satisfy the equation:

$$\int_{t_b}^t \left(\int_{t_b}^t E_s(t) dt \right) dt = 0, \quad (4)$$

Each pair of t_b and t which is related to $E_s(t)$ by Eq. (4) defines a quantum path. The sketches of electron dynamics for $\beta = 0$, $E_1 = 0$ and $\beta = 1$ are shown in Fig. 3a, c and e respectively and time-frequency analyses of the XUV spectra for $\beta = 0$, $E_1 = 0$ and $\beta = 1$ are shown in Fig. 3b, d and f respectively. For $\beta = 0$ (Fig. 3a) and $E_1 = 0$ (Fig. 3c), the electron forms three dominant quantum paths marked as R1, R2, R3 (corresponding to the middle three peaks in Fig. 3b) and S1, S2 (corresponding to the peak in Fig. 3d), S3. For $\beta = 1$ (Fig. 3e), the shape of the electric field is markedly reconstructed and three quantum paths S1, S2 and S3 (Fig. 3c) come to T1, T2 (corresponding to the left peak in Fig. 3f) and T3 (Fig. 3e).

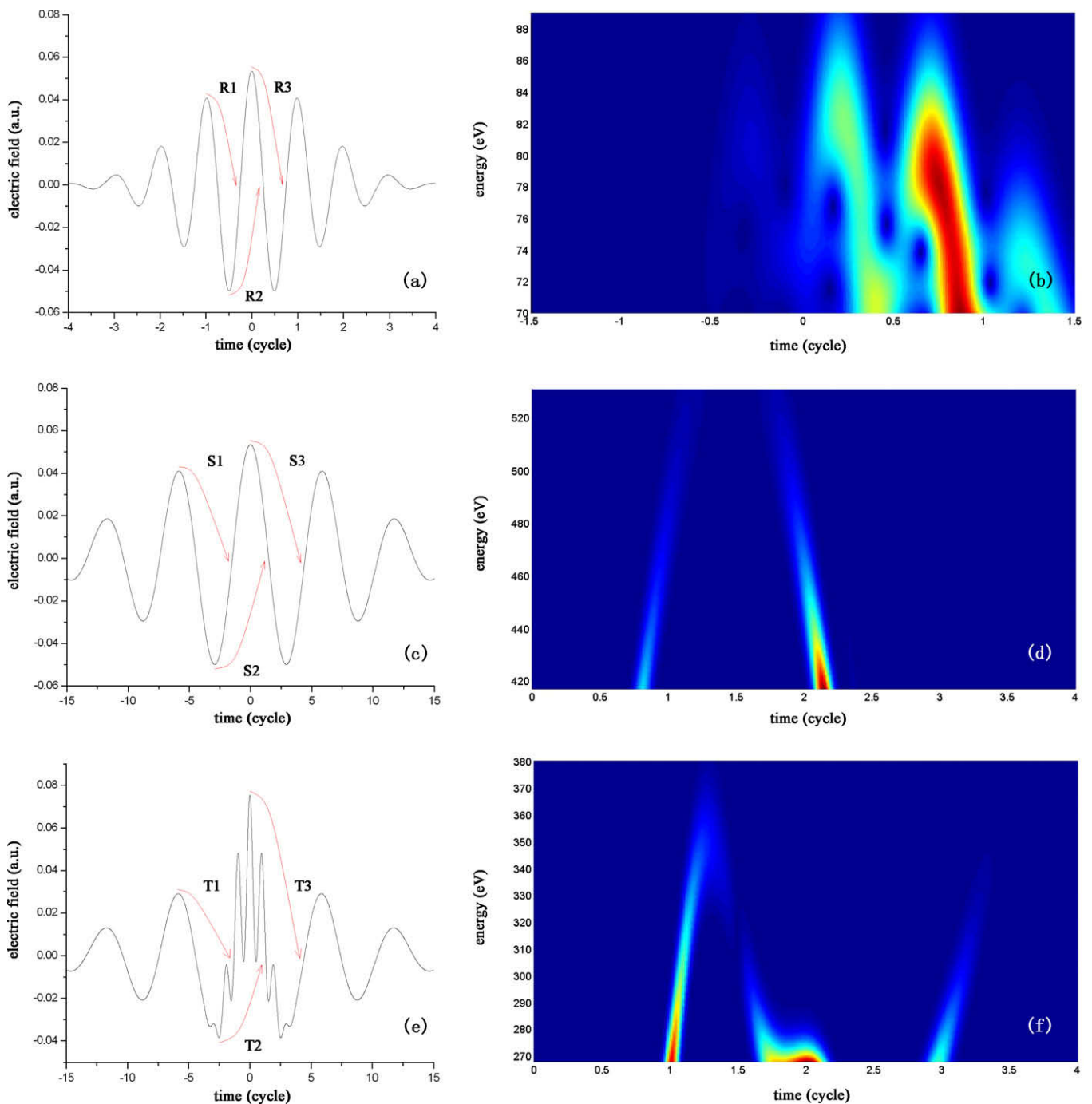


Fig. 3. (a) The sketch of electron dynamics for $\beta = 0$. (b) Time-frequency diagram of HHG for $\beta = 0$. (c) The sketch of electron dynamics for $E_1 = 0$. (d) Time-frequency diagram of HHG for $E_1 = 0$. (e) The sketch of electron dynamics for $\beta = 1$. (f) Time-frequency diagram of HHG for $\beta = 1$.

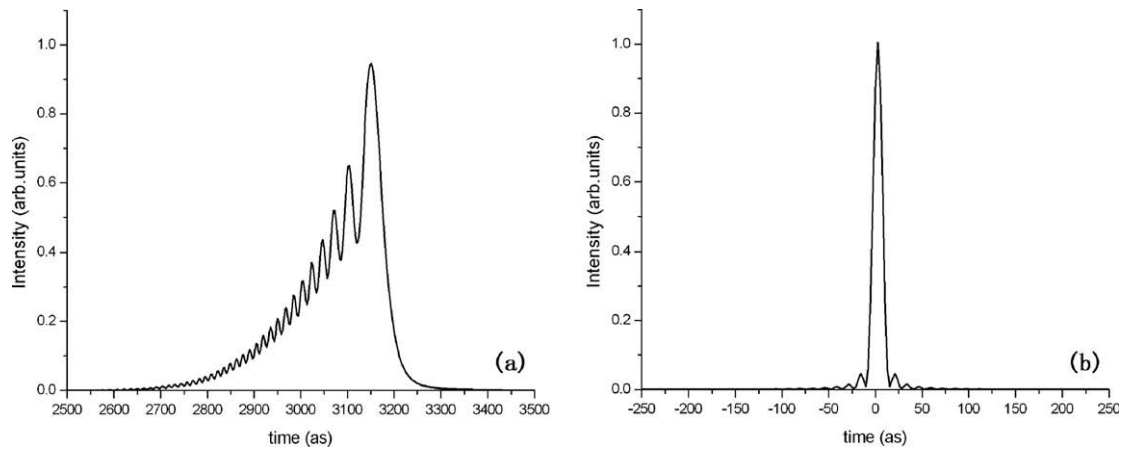


Fig. 4. (a) The temporal profiles of the single XUV pulses generated in the synthesized two-color field without phase compensation. (b) The temporal profiles of the single XUV pulses generated in the synthesized two-color field with phase compensation.

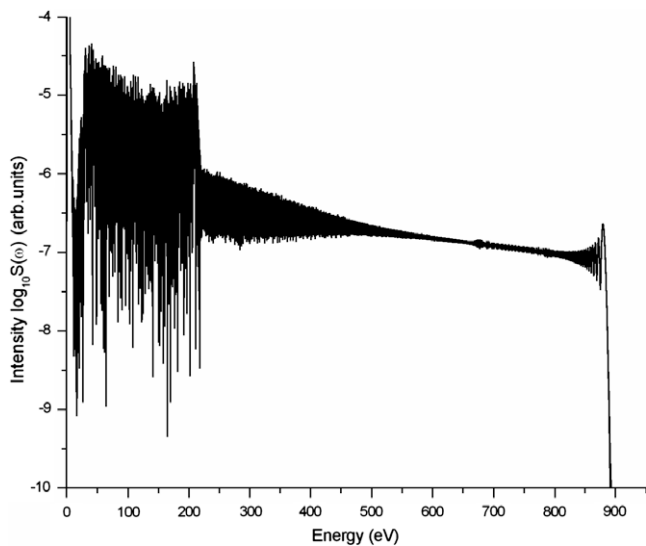


Fig. 5. The harmonic spectrum of the synthesized two-color pulse for $I_1 + I_2 = 3.0 \times 10^{14} \text{ W/cm}^2$.

When we compare Fig. 3d with Fig. 3f, we will find that in Fig. 3f the left arm (the short electron trajectory, Fig. 3d) of S2 (Fig. 3c)

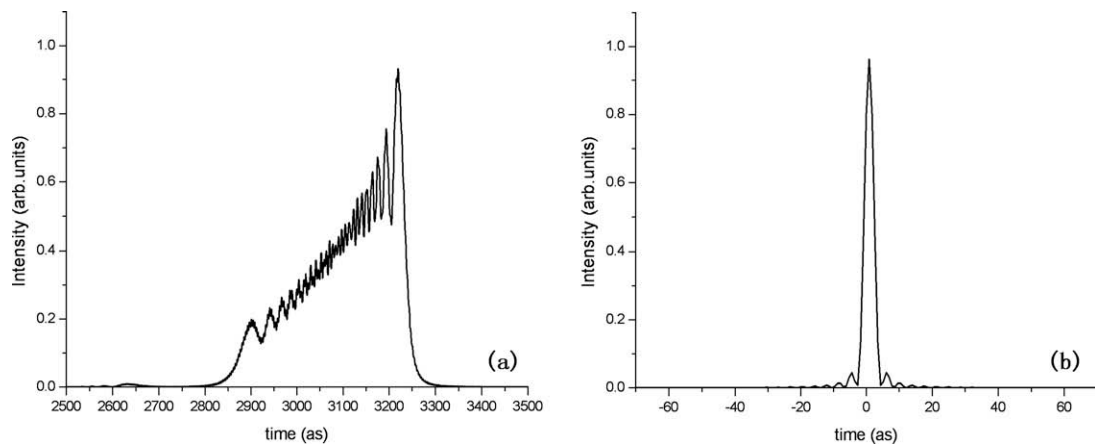


Fig. 6. (a) The temporal profiles of the single XUV pulses generated in the synthesized two-color field without phase compensation for $I_1 + I_2 = 3.0 \times 10^{14} \text{ W/cm}^2$. (b) The temporal profiles of the single XUV pulses generated in the synthesized two-color field with phase compensation for $I_1 + I_2 = 3.0 \times 10^{14} \text{ W/cm}^2$.

is enhanced while the right arm (the long electron trajectory, Fig. 3d) is restrained. As a result, we gain HHG spectrum with a small amount of spectral interference in the plateau region as shown in Fig. 2a (light gray line) and Fig. 2b (black line).

The temporal profile of the as pulse supported by the XUV supercontinuum in the range of 235–315 eV in Fig. 2a (light gray line) and Fig. 2b (black line) is calculated by a simple inverse Fourier transformation of the XUV supercontinuum, which gives out an isolated 53-as pulse without phase compensation as shown in Fig. 4a or an isolated 18-as pulse with phase compensation as shown in Fig. 4b.

If higher intensity could be achieved, such as $I_1 + I_2 = 3.0 \times 10^{14} \text{ W/cm}^2$ (remain the other parameters of the synthesized two-color pulse), a supercontinuum as long as 280 eV could be gained as shown in Fig. 5. The electron gains more energy in an intense electric field as Eqs. (2) and (3) have shown.

The XUV supercontinuum in the range of 600–880 eV (Fig. 5) gives out an isolated 28-as pulse without phase compensation as shown in Fig. 6a or an isolated 5-as pulse with phase compensation as shown in Fig. 6b.

Experimentally, our scheme can be carried out with a 10 mJ, 40 fs at 1 kHz Ti: sapphire laser system. The laser beam can be split into two beams: one is compressed to 6 fs pulses through a cascade filamentation compression technique, and another is used to produce 36 fs–4750 nm pulses via difference frequency generation (DFG).

4. Conclusion

In conclusion, we generate single attosecond pulses with well-chosen laser parameters. We choose a proper combine of driving and control pulse with low intensity to mostly modulate the electron dynamics and gain a desired HHG spectrum with high cutoff energy and a broadband flat supercontinuum cutoff region (80 eV) which supports a 53-as pulse with clean temporal profiles. We believe that this optimization algorithm can be applied in practice for XUV HHG and attosecond pulses.

Acknowledgement

This research was supported by the National Natural Science Foundation of China (Nos. 10734080 and 10574092); the National Basic Research Program “973” of China (No. 2006CB806000).

References

- [1] T. Brabec, F. Krausz, *Rev. Mod. Phys.* 72 (2000) 545.
- [2] I.J. Sola et al., *Nat. Phys.* 2 (2006) 319.
- [3] C.A. Haworth et al., *Nat. Phys.* 3 (2007) 52.
- [4] Xiaohong Song, Zhinan Zeng, Yuxi Fu, Bo Cai, Ruxin Li, Ya Cheng, Zhizhan Xu, *Phys. Rev. A* 76 (2007) 043830.
- [5] Thomas Pfeifer, Lukas Gallmann, Mard J. Abel, Phillip M. Nagel, Daniel M. Neumark, Stephen R. Leone, *Phys. Rev. Lett.* 97 (2006) 163901.
- [6] Zhinan Zeng, Ya Cheng, Xiaohong Song, Ruxin Li, Zhizhan Xu, *Phys. Rev. Lett.* 98 (2007) 203901.
- [7] Y. Oishi, M. Kaku, A. Suda, F. Kannari, K. Midorikawa, *Opt. Express* 14 (2006) 7230.
- [8] Weiyi Hong, Peixiang Lu, Pengfei Lan, Zhenyu Yang, Yuhua Li, Qing Liao, *Phys. Rev. A* 77 (2008) 033410.
- [9] Wei Cao, Peixiang Lu, Pengfei Lan, Xinlin Wang, Yuhua Li, *Phys. Rev. A* 75 (2007) 063423.
- [10] Pengfei Lan, Peixiang Lu, Wei Cao, Yuhua Li, Xinlin Wang, *Phys. Rev. A* 76 (2007) 011402.